

Real-Time Diode Laser Measurements of Vapor-Phase Benzene

J. D. Jeffers, C. B. Roller, and K. Namjou

Ekips Technologies, Inc., Norman, Oklahoma 73069

M. A. Evans, L. McSpadden, J. Grego, and P. J. McCann*

School of Electrical and Computer Engineering, University of Oklahoma, Norman, Oklahoma 73019

An absorption spectrometer equipped with a IV–VI semiconductor tunable mid-IR diode laser was used to make sensitive measurements of benzene (C₆H₆) gas in the 5.1- μ m spectral range. Wavelength modulation coupled with second-harmonic detection achieved accurate real-time quantification of benzene concentrations down to a minimum detection limit of 1 ppmv with an integration time of 4 s. A variety of calibrated benzene-sensing measurements were made, including the determination of the benzene concentrations in vehicle exhaust and headspace vapors from unleaded gasoline and other liquids. Kinetic phenomena, including the monitoring of benzene evaporation and absorption/desorption by granulated activated carbon were observed with the instrument. Measurements were performed that allowed experimental determination of the activation energy for desorption of benzene from activated carbon, which was found to be 198 meV/molecule (19.0 kJ/mol).

Benzene (C₆H₆) is a volatile organic compound that is a known carcinogen with an established link to an increased risk of leukemia.¹ Various reports have cited occupational exposure to benzene along with its derivative family, BTEX (benzene, toluene, ethylene, xylene), at petroleum refineries, styrene plants, shoe-making factories, and waste incineration sites. Between 1 and 50 ppm levels of benzene are also found in tobacco smoke, gasoline vapors, and automobile exhaust. The National Institute of Occupational Safety and Health (NIOSH) recommends exposure levels of no more than 0.1 part per million (ppm) air, while the Occupational Safety and Health Administration (OSHA) has set the legally enforceable limit at 1 ppm averaged over an 8-h workday.

Mass spectroscopy coupled with gas chromatography (GC/MS) is the most widely used nonoptical method for detecting benzene concentrations in liquid or gas samples. GC/MS, however, is effectively limited to laboratory use by a skilled technician because of the difficulty of sample introduction and instrument operation. Various nondestructive optical gas-sensing methods have been used to measure benzene trace gases, including Fourier transform infrared (FT-IR) spectroscopy² and tunable diode laser

absorption spectroscopy (TDLAS) using mid-IR IV–VI diode lasers^{3,4} or difference-frequency-generated (DFG) mid-IR light sources.⁵ Other laser-based detection methods, including differential absorption lidar (DIAL) and photoacoustic spectroscopy, have also been used to make sensitive benzene measurements in various spectral regions. FT-IR spectrometers can effectively scan continuously over several thousand wavenumbers in the mid-IR spectral “fingerprint” region, providing for measurements of many molecular species simultaneously. FT-IR has been used to measure benzene with sub-parts-per-million sensitivities;⁶ however, low-resolution (typically ≥ 0.5 cm⁻¹) and low-mid-IR broadband source optical powers necessitate long integration times on the order of several minutes. FT-IR is also susceptible to interference from high concentrations of H₂O, CO₂, and other molecules in ambient air. Elevated relative humidity and presence of other hydrocarbons further complicate precise measurements.

Laser-based photoacoustic spectroscopy techniques achieve high sensitivity by exciting atoms at a single wavelength with a high power beam and detecting the resulting periodic pressure changes with a microphone. Using a CO₂ laser at 9.6392 μ m, a minimum detection limit of 3 ppb has been reported for benzene.⁷ CO laser spectroscopy has been used to measure benzene concentration in the exhaust of several vehicles.⁸ However, these lasers lack the capability to continuously scan over a spectral region. In gas mixtures, there is often more than one species that absorbs at a particular infrared wavelength, and this interference makes it difficult to distinguish the component of interest from other components. Alternatively, DIAL detection methods transmit laser pulses into the atmosphere and detect backscattered radiation. Using a frequency-doubled dye laser source at 253 nm with a DIAL detection scheme, benzene measurements have been reported with a minimum detection limit of 8 ppb.⁹

(2) Schaefer, K.; Emeis, S. M.; Stackhouse, M.; Sedlmaier, A.; Hoffmann, H.; Depta, G. *Proc. SPIE, Environ. Monit. Rem. Technol.* **1999**, 3534, 212–219.

(3) Waschull, J.; Sumpf, B.; Heiner, Y.; Kronfeldt, H.-D. *Infrared Phys. Technol.* **1996**, 37, 193–198.

(4) Berger, J.; Pustogov, V. P. *Infrared Phys. Technol.* **1996**, 37, 163–166.

(5) Chen, W.; Cazier, F.; Tittel, F.; Boucher, D. *Appl. Opt.* **2000**, 39, 6238–6242.

(6) Hren, B.; Katona, K.; Mink, J.; Kohan, J.; Isaak, Gy. *Analyst* **2000**, 125, 1655.

(7) Kreuzer, L. B.; Kenyon, N. D.; Patel, C. K. N. *Science* **1972**, 177, 347–349.

(8) Bernegger, S.; Sigrist, M. W. *Infrared Phys.* **1990**, 30, 375–427.

* Corresponding author. E-mail: pmccann@ou.edu.

(1) Snyder, R. *Crit. Rev. Toxicol.* **2002**, 32, 155.

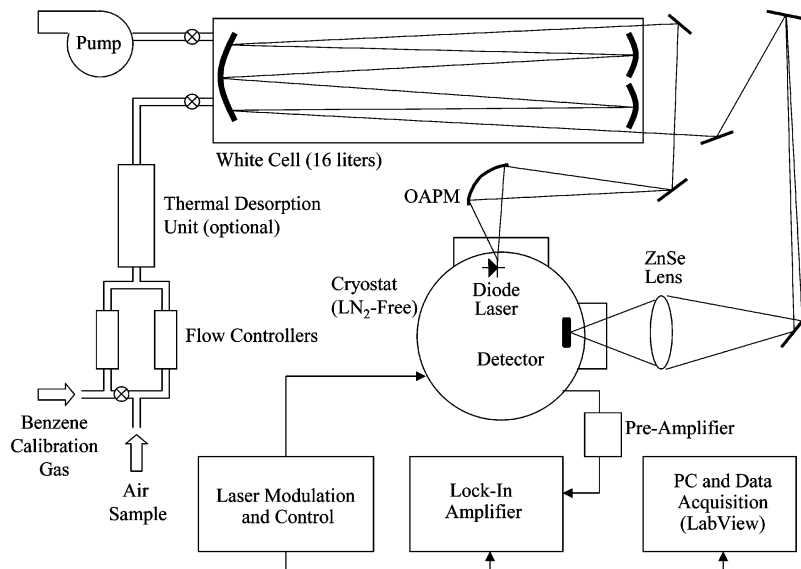


Figure 1. TDLAS experimental setup showing cryostat with laser and detector, off-axis parabolic mirror (OAPM), gas cell, flow controllers, thermal desorption unit, electronics, and computer for instrument control and data acquisition.

TDLAS sensors equipped with IV–VI lasers have high spectral resolution (typically $<0.001\text{ cm}^{-1}$), high optical output power (2 mW maximum, typically $\sim 300\text{ }\mu\text{W}$), single frequency mode emissions, and wide tunability (typically $1\text{--}3\text{ cm}^{-1}$). Instruments equipped with IV–VI lasers have achieved sub-parts-per-billion (ppb) sensitivities, provide response times of $<1\text{ s}$, and possess the ability to measure several trace gas species simultaneously.^{10,11} Using a laser with emission at $14\text{ }\mu\text{m}$ and a 3.46-m optical path, a benzene detection limit of 80 ppm was estimated on the basis of measurements of a 200 ppm benzene sample and a signal-to-noise ratio (SNR) of 1.⁴ Employing a laser with emission at $10\text{ }\mu\text{m}$ and a 45-m optical path allowed a benzene detection limit of 1 ppm to be calculated using experimentally determined line strengths and pressure-broadening coefficients.⁴ A theoretical detection limit of 2 ppb was calculated for benzene measurements at $15\text{ }\mu\text{m}$ using a 132-m multipass cell at 10 Torr and a 1-s integration time.¹² In addition, an absorption spectrometer equipped with a DFG mid-IR laser having emission in the $14.8\text{-}\mu\text{m}$ spectral range and a 10-cm-long gas cell was used to measure a 173.1 ppm benzene gas sample.⁵ The resulting SNR suggested a minimum benzene detection limit of 11.5 ppm.

Until recently, the $5\text{--}8\text{-}\mu\text{m}$ region has not been extensively utilized to measure vapor-phase benzene. This spectral region contains a broad H_2O absorption band located approximately between $1300\text{ and }1990\text{ cm}^{-1}$, and the benzene absorption bands in this region are less pronounced when compared to bands at other wavelengths. However, the narrow line widths of the IV–VI diode laser combined with a low-pressure gas cell in the TDLAS system can provide adequate resolution to identify unambiguous benzene absorption features without interference from H_2O , CO_2 , and NO , which exhibit absorption lines in this spectral range.

This paper describes the development and use of a mid-infrared TDLAS system designed specifically for benzene measurements. This optical sensor technology offers the benefits of high sensitivity, high selectivity, and rapid response times. High sensitivity is demonstrated by measuring a calibrated (100 ppm) benzene gas standard serially diluted down to 1 ppmv. High selectivity is demonstrated by the detection of benzene specific absorption features in multicomponent gas mixtures. Rapid response times are demonstrated by real-time monitoring of various gas evaporation, absorption, and desorption phenomena. In addition to describing practical benzene sensing applications, this paper also includes experimental results obtained from sorption of benzene onto granular activated carbon and subsequent desorption at different temperatures. These measurements provide a real-time view of the various steps of a thermal desorption unit, which is often coupled with GC/MS instruments to concentrate gaseous samples. Results from this work also include the derivation of the activation energy required to desorb benzene from granular activated carbon.

TDLAS Instrumentation. Hardware and Software. The experimental setup is shown in Figure 1. A temperature-controlled stage inside a sealed cryostat was used to mount a double heterostructure IV–VI semiconductor mid-infrared laser and HgCdTe photovoltaic detector. An integrated heater, mounted just beneath the laser mount, and a closed-cycle cryogenic refrigerator maintained stable operating temperatures between 77 and 115 K without liquid nitrogen consumption. The temperature controller (Lakeshore, Westerville, OH) maintained constant temperatures within $\pm 0.01\text{ K}$. Various optical mirrors and a meniscus lens were used to direct and collimate the laser beam exiting through a ZnSe window in the cryostat through a 107-m White cell (Infrared Analysis, Anaheim, CA, model no. 107-V) and back through another ZnSe window onto the photovoltaic detector.

Sweep integration coupled with wavelength modulation for 2f detection was implemented with a triangle waveform (23–36 kHz) superimposed onto a 40-Hz sawtooth waveform. The detector signal was preamplified and sampled at twice the modulation

- (9) Milton, M. J. T.; Woods, P. T.; Jolliffe, B. W.; Swann, N. R. W.; McIlveen, T. *J. Appl. Phys. B* **1992**, *55*, 41–45.
 (10) Roller, C. B.; Namjou, K.; Jeffers, J.; Potter, W.; McCann, P. J.; Grego, J. *Opt. Lett.* **2002**, *27*, 107.
 (11) Roller, C. B.; Namjou, K.; Jeffers, J.; Camp, M.; McCann, P. J.; Grego, J. *Appl. Opt.* **2002**, *41*, 6018.
 (12) Sigrist, M. W. *Chemical Analysis Series: Air Monitoring by Spectroscopic Techniques*; Wiley: New York, 1994; p 281.

frequency with a lock-in amplifier (Stanford Research Systems, Sunnyvale, CA, model no. SR830) to obtain second-harmonic ($2f$) spectra. A scan of either 500 or 1000 data points was uploaded from the output of the lock-in amplifier to memory for postprocessing on a personal computer through an analog-to-digital converter.

A running coverage of the previous 75 scans was maintained and displayed using a custom graphical user interface (GUI) software program. A software "line-locking" routine was used to address absorption spectra shifting due to slight thermal variations of the laser. An unambiguous peak corresponding to an H_2O absorption line in the acquired spectrum was used to align each spectrum before co-adding to reduce smear. Subsections of acquired spectra with benzene absorption features were compared online to a calibrated reference spectrum using a linear least-squares fitting routine.¹³ The system achieved a measurement integration time of ~ 4 s for 75 co-added scans.

A mechanical pump reduced the gas cell pressure to the 5–30 Torr range and induced a flow of 1.0 L/min held constant with mass flow controllers. The low-pressure 16 L White cell and high flow rates allowed continuous flow measurements, with a typical clearance time of < 2 s, shorter than the 4-s software integration time. Teflon, stainless steel, and copper tubing and fittings were used for all connections in the gas sampling apparatus.

The thermal desorption sample introduction stage was assembled from parts removed from a Tekmar (Cincinnati, OH) model 5010 thermal desorption unit. It consisted of a stainless steel tube, enclosed by a heating unit, placed in series between the outlet of the flow controllers and the inlet of the gas cell. The 7-in.-long 5/8-in.-diameter trap was filled with 6.7 g of granular activated carbon held in place by DMCS (dimethyl dichlorosilane)-treated glass wool at both ends. The granular activated carbon was sieved to provide a particle range of 5 mm to 1 mm. A temperature controller, model no. 6080-F0-A (Athena, Plymouth Meeting, PA), was used to heat the trap at ~ 100 °C/min and to maintain a constant final desorption temperature of up to 400 °C, as measured with a type K thermocouple that was integrated with the Tekmar heating coil.

Benzene Spectral Features and Midinfrared Laser Emission. TDLAS is most commonly applied to spectroscopic measurements of small molecules, such as H_2O and NO , whose absorption line features can be found in the HITRAN database.¹⁴ These small molecules typically have widely spaced rotational–vibrational (rovibrational) absorption lines, which can be resolved with narrow line width mid-IR lasers. Mid-IR absorption bands for larger molecules, such as BTEX compounds, have been measured with FT-IR spectroscopy or obtained theoretically.^{15,16} These absorption bands actually consist of numerous closely spaced rovibrational absorption lines, which are typically not resolved with low-resolution FT-IR instruments. Prior work¹⁷ has shown that it is possible to tune a mid-IR laser across a 150-cm^{-1}

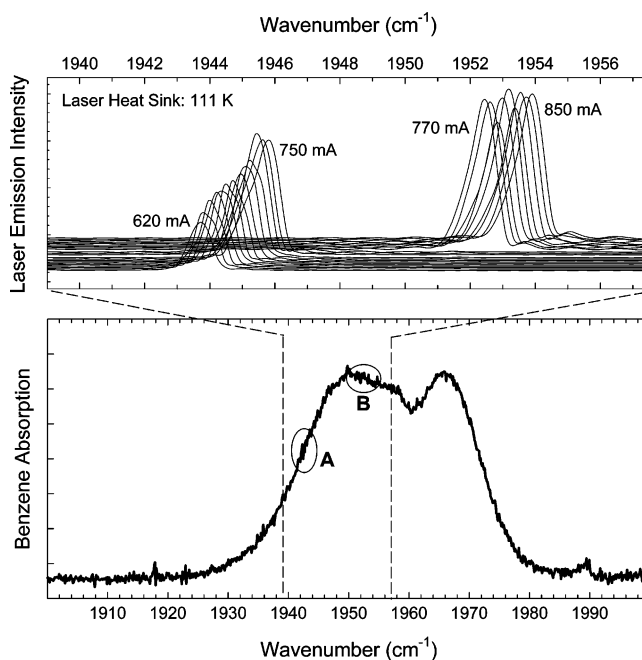


Figure 2. Benzene absorption spectrum, as measured with a 0.5-cm^{-1} resolution FT-IR, and laser emission spectra in the same region for various injection currents with a laser heat sink temperature of 111 K. Spectral line widths of the laser emission is typically $< 0.001\text{ cm}^{-1}$, much smaller FT-IR instrument resolution limited spectra displayed here. This laser allowed measurement in two spectral regions, marked by A and B of the benzene ring overtone band.

spectral range or more by ramping the laser heat sink temperature and obtaining a dc offset in the transmitted light intensity corresponding to broad absorption bands for benzene and toluene. This technique, however, suffers from the disadvantage of requiring long measurement times of ~ 10 min or more. Alternatively, faster detection can be accomplished by rapid tuning (using an injection current ramp) across a smaller spectral region to scan resolvable rovibrational absorption features that are unique to the benzene molecule. Individual rovibrational absorption lines for benzene have been measured in the $6.7\text{-}\mu\text{m}$ ν_{13} band using jet expansion cooling.¹⁸ Jet expansion cooling was not employed for this work; thus, absorption line features are much more dense, and any resolvable features will likely be a combination of several absorption lines.

Figure 2 shows the $5.1\text{-}\mu\text{m}$ ($1930\text{--}1980\text{ cm}^{-1}$) absorption spectrum for a benzene ring overtone band obtained with a low resolution (0.5 cm^{-1}) FT-IR spectrometer along with measured emission intensities (also obtained with a 0.5 cm^{-1} resolution FT-IR spectrometer) for the mid-IR laser that was used in the experiments described here. This laser exhibited strong (up to 2 mW continuous wave) single-mode emission in several different spectral regions, including the 1943 and 1952 cm^{-1} regions, indicated by the letters A and B on the benzene ring overtone absorption band. For a laser heat sink temperature of 111 K, the lower frequency range was obtained by varying injection currents between 620 and 750 mA, whereas the higher frequency range was obtained by varying injection currents between 770 mA and 850 mA. Note that the spectral width of the laser emission is

(13) Fried, A.; Drummond, J. R.; Henry, B.; Fox, J. *Appl. Opt.* **1991**, *30*, 1916–1932.

(14) Rothman, L. S., et al. *J. Quant. Spectrosc. Radiat. Transfer* **1998**, *60*, 665–710.

(15) Dang-Nhu, M.; Pliva, J. *J. Mol. Spectrosc.* **1989**, *138*, 423–429.

(16) Kauppinen, J.; Jensen, P.; Brodersen, S. *J. Mol. Spectrosc.* **1980**, *83*, 161–174.

(17) McCann, P. J.; Namjou, K.; Roller, C.; Jeffers, J.; Debebe, Z.; Grego, J.; *Proc. SPIE, Environ. Indust. Sensing* **2001**, *4574*, 201–207.

(18) Uskola, A.; Basterretxea, F. J.; Castano, F. *J. Mol. Spectrosc.* **1999**, *198*, 429.

actually much narrower ($<0.001\text{ cm}^{-1}$) than what is shown in Figure 2. In addition, these data are for operation of the laser with a static (dc) injection current. During spectroscopic measurements, when the laser is operating in a dynamic mode with an above-threshold current ramp, there will be additional heating of the laser active region, and this effect can be accounted for by using data for a lower heat sink temperature when matching the dynamic tuning case to the static dc test data case. It was found that laser heat sink temperatures of 109 and 110 K, when in a dynamic tuning mode of operation, produced tuning ranges similar to those for a heat sink temperature of 111 K, as shown in Figure 2.

Gas Sampling Procedures. Quantitative benzene gas measurements were performed using NIST traceable calibration gas containing $100\text{ ppm} \pm 2\%$ benzene balanced with N_2 (Airgas South, Mobile, AL). Two flow controllers were used to serially dilute the 100 ppm benzene to concentrations down to 1 ppmv by mixing with nitrogen or laboratory air. Calibrated measurements of various air samples were performed by using a reference spectrum that corresponded to a 10 ppmv or 50 ppmv benzene sample flowing through the gas cell. New reference spectra were generated weekly with this 100 ppm calibration gas, and it was found that the overall system was very stable, with only small changes ($<10\%$) in the intensities of absorption features for benzene in the reference spectra.

Air samples containing benzene were collected and measured using a variety of methods. For collection of air samples from sources such as automobile exhaust and gasoline headspace vapors, a 6-L stainless steel container (Summa Canister) with separate inlet and outlet valves was used to collect and transport air samples to the laboratory. Between uses, the canisters were purged with N_2 gas and evacuated to a pressure of <0.5 Torr three times to eliminate carryover. The canister was equipped with an 18-in.-long 1/4-in.-o.d. Teflon tube inlet that allowed collection of gas samples from automobile tailpipes and headspace vapors inside fuel tanks. Air samples were acquired by opening the inlet valve for ~ 10 s, which filled the evacuated canister to atmospheric pressure. Three separate canisters were used to acquire atmospheric background and multiple source samples. Collected air samples were transferred to the 16-L White cell by first evacuating it to <0.5 Torr then filling it to the operating pressure of 10 Torr with gas from the canister. For continuous monitoring of laboratory air samples, a 0.25-in.-o.d. Teflon tube was connected to the inlet of the flow controllers, allowing the gas to flow directly into the reduced pressure gas cell and out through the mechanical pump.

Thermal desorption experiments were performed by allowing air samples to flow through the granulated activated carbon, which was held at room temperature, and through the White cell at a flow rate of 1.0 L/min. After a 7–10-min period of absorption by the carbon, the valve between the desorption unit and the White cell was closed, and the flow controllers were turned off. This allowed the White cell to be evacuated, and when it reached a pressure of 0.3 Torr, the valve between the White cell and the mechanical pump was closed, and the desorption unit was heated to a specified temperature. After heating for 5 min, the gas cell inlet was opened, allowing the desorbed benzene to flow into the evacuated cell. The final gas cell pressure and benzene concentra-

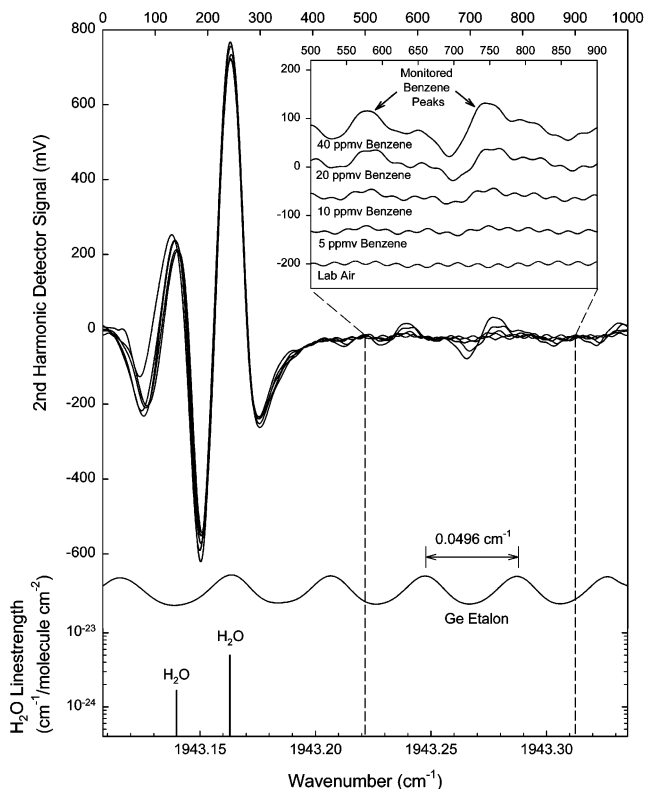


Figure 3. Second harmonic laser absorption spectra in the 1943.1–1943.3- cm^{-1} range (Region A) for various gas samples containing different concentrations of benzene vapor. The germanium Etalon spectrum is used to calibrate the spectral scale. The strong H_2O absorption line near 1943.16 cm^{-1} is used to “lock” the laser onto this spectral region.

tion were recorded. Before subsequent measurements, any remaining benzene was purged from the system by heating the trap to $300\text{ }^\circ\text{C}$ while flowing lab air through the system at 1.0 L/min for ~ 20 min.

RESULTS

Figure 3 shows TDLAS absorption spectra between 1943.1 and 1943.3 cm^{-1} (region A in Figure 2) for lab air and air samples containing 5, 10, 20, and 40 ppmv benzene. This spectral region was identified with the aid of two absorption lines for water near 1943.15 cm^{-1} , whose exact frequencies were obtained from the Hitran database. The laser heat sink temperature was 109 K, and the laser injection current was nominally 700 mA with a 50 mV peak-to-peak voltage ramp to the current source modulation input. Also shown is a spectrum for a 1-in.-thick germanium Etalon with a free spectral range of 0.0496 cm^{-1} . This was used to calibrate the wavenumber scale for the spectra. The channel numbers for the digitally captured spectra are shown on the top scale. Two absorption features associated with rovibrational modes of benzene are clearly seen in the vicinity of 1943.25 cm^{-1} . The inset shows an expanded view of these two dominant absorption features, which are still apparent in the 5 ppmv spectrum. The existence of closely spaced Etalon fringes is due to TDLAS system optics. The free spectral range of 0.0081 cm^{-1} corresponds to a physical distance of 62 cm in air, which is very close to the distance between the off-axis parabolic collimating mirror for the laser and

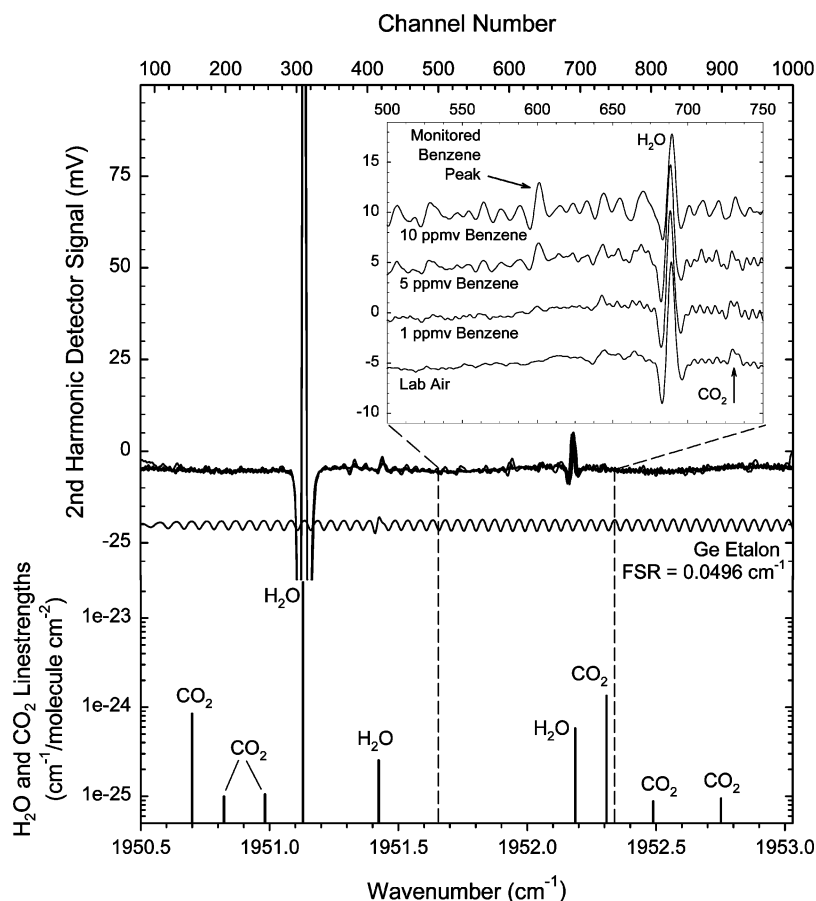


Figure 4. Second harmonic laser absorption spectra in the 1950.5–1953.0- cm^{-1} range (Region B) for various gas samples containing different concentrations of benzene vapor. Several strong absorption features having a pattern uniquely associated with benzene are observed near 1952 cm^{-1} . Strong H_2O absorption lines and a CO_2 line representing the ambient concentration of ~ 365 ppm are also observed.

the CaF_2 window on the White cell. These Etalon fringes are the primary limit of system performance in laser absorption spectrometers.

Figure 4 shows TDLAS absorption spectra between 1950.5 and 1953.0 cm^{-1} (region B in Figure 2) for lab air and air samples containing 1, 5, and 10 ppmv benzene. This spectral region contains numerous individually resolvable absorption lines for H_2O and CO_2 along with clearly identifiable absorption features associated with benzene. The laser heat sink temperature was 110 K, and the laser injection current was nominally 740 mA with a 500 mV peak-to-peak voltage ramp to the current source modulation input. Note the much wider spectral coverage range, due to the larger voltage ramp, as compared to Figure 3 and indicated by the larger number of fringes from the germanium Etalon. Although the nominal injection current is nearly the same as what is shown in Figure 2 for this spectral coverage, the laser heat sink temperature is 1° less, indicating that the current tuning ramp increases the active region temperature by about this amount. (The laser operating parameters for region A are 2° less than what is shown in Figure 2, but the nominal injection current is higher, which causes the laser to tune in a higher frequency region.) A peak corresponding to the strongest CO_2 absorption line in this spectral region near 1952.3 cm^{-1} was observed in ambient laboratory air samples. This peak, which represents the current atmospheric CO_2 concentration value of 365 ppm, increased significantly when a 5% CO_2 gas sample was flowed through the cell.

Benzene concentration trends for the two different spectral regions were made by adjusting the concentration to various values between 0 and 20 ppm for ~ 5 -min intervals. These trend data, which show concentration values every 4 s, exhibit noise spikes that correspond to a concentration value of ~ 1 ppmv. Benzene concentrations of 3 and 1 ppmv are detectable for both the A and B spectral regions, respectively. Measurements of diluted concentrations of benzene from 3 to 100 ppm in spectral region B were linear with an R^2 value of 0.9997. The minimum detection limit was obtained by measuring the V_{rms} noise signal for a gas sample of nitrogen only and multiplying this value by 3 to get a corresponding concentration value of 1 ppmv, which is similar to the noise spikes observed in the trends. There was no significant difference in minimum detection limits for the two different spectral regions measured. This is despite region B's being in a much stronger portion of the benzene absorption band.

Three sets of experiments were conducted to illustrate the benzene detection capabilities of the TDLAS system. First, headspace vapors from various liquids and automobile exhaust from two vehicles were tested for benzene concentration. Second, the decay of benzene vapor concentration over a single drop of evaporating benzene was examined. Finally, the desorption of benzene from activated carbon was studied through use of the thermal desorption unit.

The detection of vapor-phase benzene over the headspace of various liquids illustrates the ability of the system to selectively measure benzene in the presence of large concentrations of other

Table 1. Measured Benzene Concentrations from Various Air Samples

measured air sample	benzene concn, ppm
acetone headspace	<1
toluene headspace	<1
laboratory air	<1
methanol headspace	20
gasoline headspace	55
SUV exhaust	2.6
motorcycle exhaust	2.3

species. Headspace vapors from liquid toluene and acetone were sampled, and in both cases, there were no observable absorption features in the spectral regions scanned. The effect of toluene was observable only when the concentration was extremely high (>1%), at which point it changed the shape of the H₂O absorption feature. On the other hand, headspace vapors collected over liquid methanol (Fisher Scientific, optima grade) showed the same unique absorption feature pattern as the reference spectrum, with peak heights corresponding to benzene concentrations in the 20 ppmv range. In addition, ambient laboratory air samples drawn continuously through the system as well as air samples drawn from a nearby parking lot showed no benzene above the 1 ppmv detection limit.

To show that the TDLAS system can be used to monitor OSHA limits in samples collected from the field, vapors from various locations were collected and analyzed. Samples collected from the headspace vapor over a 91-octane gasoline sample, the exhaust of a 1998 fuel-injected 6-cylinder sport utility vehicle (SUV), and the exhaust of a 2002 fuel-injected 4-cylinder 600 cm³ motorcycle all showed detectable levels of benzene, which are given in Table 1 along with results from the headspace vapors and air samples discussed above. Both engines were equipped with catalytic converters and used 91-octane commercial gasoline under idling conditions. Each sample was introduced into the gas cell and analyzed (integration time of 5–10 s, depending on computer load) for 5 min to obtain a multipoint concentration trend. This trend was then postprocessed to yield the mean and standard deviation for benzene. The spectra for these samples showed the same unique pattern of absorption features as the reference spectrum for benzene in nitrogen, thus providing substantial confirmation that these air samples indeed contained benzene. The headspace vapor over gasoline had a benzene concentration of 55.0 ± 0.4 ppm, more than 50 times the OSHA 8-h permissible exposure limit (PEL), while benzene concentrations in SUV and motorcycle engine exhaust were 2.58 ± 0.02 ppm and 2.33 ± 0.02 ppm, respectively, both more than 2 times the OSHA PEL.

An example of the real-time and fast-response sensing capabilities of this TDLAS method is shown in Figure 5, which is a concentration trend during a 1.5-h period of benzene vapor in air over a single drop of liquid benzene placed in the bottom of a 225-mL Erlenmeyer flask. Air was continuously sampled through the inlet of the 0.25-in-diameter Teflon tube located ~2 cm above the center of the flask's mouth. The benzene concentration immediately spiked to above 250 ppmv, declined to ~20 ppmv after ~1 min, then rose again to ~150 ppmv, at which time an exponential decrease in the concentration was observed. The evaporation trends for single drops of benzene were quite

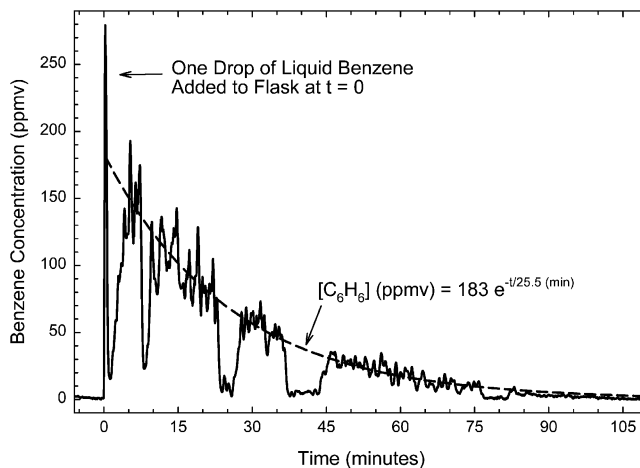


Figure 5. Trend showing benzene vapor concentration, with an exponential fit, over an evaporating drop of benzene placed inside a 225-mL flask. Benzene concentration stayed well above 1 ppmv for more than 1 h. Decreases in benzene concentrations at 8, 25, 40, and 80 min are due to air flow generated by a corona discharge air cleaner device, which was found to be ineffective in decomposing benzene. Measurements were made in spectral region B.

repeatable, including the high concentration spike at the beginning of the trend. A fit to the data showed a time constant of 25.5 min, which is attributed to the diffusion of benzene vapor out of the flask from the limited source of a single liquid drop as it evaporates. At four different times during this evaporation process (~8, 25, 40, and 80 min) a small battery-powered corona-discharge air-cleaning device (Wein Products, Los Angeles, CA) located near the air sample inlet was turned on and off. Each time, the benzene concentration decreased significantly, but this effect was due to an air flow effect rather than a chemical decomposition effect, as confirmed by sampling at different locations along the slight flow of air generated by the air cleaner unit, which showed that the benzene vapor was being blown across the mouth of the flask before it could reach the inlet.

Benzene concentration trend data shown in Figure 6 provide another example of the real-time benzene detection capabilities of TDLAS technology and illustrate a possible method for improving instrument sensitivity. The first 13 min shows 10 ppmv benzene then lab air flowing through the system, which included the thermal desorption unit without the trap. At 25 min, after the trap was placed in the thermal desorption unit, lab air was flowed, followed by 10 ppmv benzene. No increase in benzene concentration in the gas cell downstream from the trap was observed, indicating that benzene was being completely absorbed during this 7-min period. Similar experiments using zeolite as the absorbent showed no decrease in benzene concentration, indicating that zeolite is not an effective benzene-trapping material. Subsequent heating of the trap up to 150 °C while flowing lab air at 1.0 L/min through the system did not release a significant amount of benzene, whereas heating to 250 °C released ~10 ppmv benzene for several minutes. Further heating to 300 °C produced a peak of 20 ppmv, followed by an exponential decay. Increasing the temperature to 400 °C released no more benzene. Further thermal desorption experiments were conducted to examine the kinetics of benzene desorption from activated carbon in real-time. Benzene vapor from a drop of liquid benzene in an Erlenmeyer flask was allowed to flow through the thermal desorption unit

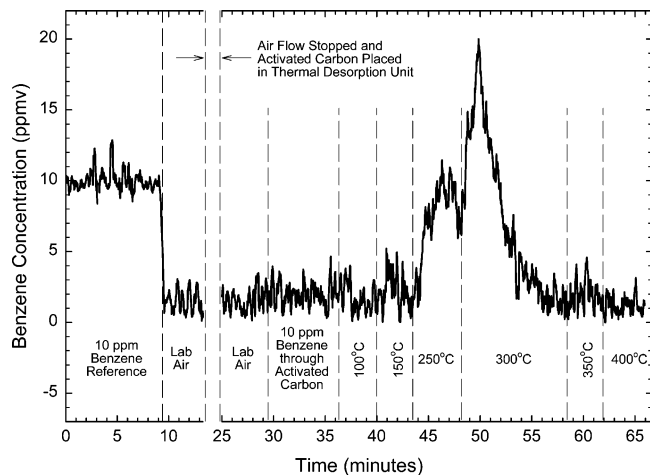


Figure 6. Benzene concentration trend showing flow of 10 ppmv sample without activated carbon in path, flow of 10 ppmv sample with activated carbon in path, and thermal desorption from the activated carbon at different temperatures. A 10-min desorption at 300 °C is sufficient to remove benzene from carbon, as evidenced by lack of additional benzene desorption at higher temperatures.

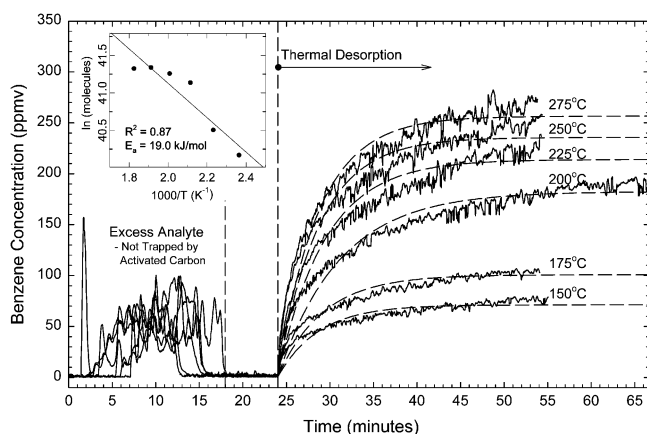


Figure 7. Multiple benzene concentration trends showing flow of ~100 ppmv benzene through 6.7 g of activated carbon at room temperature and subsequent thermal desorption, with exponential fits, at different temperatures. In each case, the activated carbon was completely saturated, as indicated by the excess benzene during the absorption process in the 0–18 min time frame. Note the concentration spike at the 2-min point in one of the trends. This is similar to what is shown in Figure 5. Inset shows an Arrhenius plot of quantity of desorbed benzene versus inverse temperature. The slope of the linear least-squares fit yields an activation energy of 198 meV/molecule for benzene desorption from activated carbon.

packed with activated carbon. These vapors were collected for the first 10 min of evaporation. The average benzene concentration during this time, based on data in Figure 5, was 100 ppmv. This was a sufficient concentration to saturate the granular activated carbon, as indicated by the concentration trends in Figure 7, which show the absorption and thermal desorption steps. Six different runs showed fairly consistent concentrations of unabsorbed analyte with concentrations of excess benzene ranging from 37.3 to 53.4 ppmv. Subtracting the mean of these values from the 100 ppmv average benzene concentration that was exposed to the activated carbon yields an absorbed concentration of 55 ppmv, or 22.5 μmol of total benzene analyte over the 10-min period. Therefore, the room-temperature saturation level, or maximum load, for benzene in granulated activated carbon is 40.3 ppm (using

Table 2. Data for Thermal Desorption of Benzene from Activated Carbon

desorption temp (°C)	final gas cel pressure (Torr)	benzene concn (ppmv)	benzene released (μmol)
150	7.57	71	0.463
175	7.44	101	0.647
200	7.72	183	1.22
225	7.45	214	1.37
250	7.33	236	1.48
275	6.63 ^a	257	1.47

^a The lower gas cell pressure for the higher desorption temperatures is likely due to a system leak in the thermal desorption unit.

the 6.7 g mass of activated carbon in the trap). The trends, beginning at 25 min, show the release of absorbed benzene from the saturated carbon into the evacuated gas cell for various desorption temperatures. Exponential fits to the measured concentration trends were used to obtain final asymptotic values for the different benzene concentrations. Table 2 summarizes results from these thermal desorption experiments. The inset in Figure 7 shows a plot of the log of benzene molecules vs $1/T$, showing an Arrhenius equation fit with an R^2 value of 0.87. These data revealed an activation energy of 198 meV/molecule (19.0 kJ/mol) for desorption of benzene from carbon.

DISCUSSION

The results described above show benzene vapor in air samples can be quantifiably measured using TDLAS instrumentation with a minimum detection limit of 1 ppm, >10 times better than the best reported detection limit up until now for a TDLAS measurement.⁵ The real-time and autonomous nature of the measurement makes this analytical method ideally suited for unattended continuous monitoring of air quality where occupational exposure to benzene vapors may be a possibility. Although the system described here is bulky and impractical for field use, new gas cell technology, such as much more compact astigmatic multipass Herriott cells, can enable significant reductions in instrument size. Improvements in the minimum detection limit to below 1 ppm should be possible with longer sample integration times. All measurements performed here had short sample integration times of ~4 seconds. Performing a running co-average of measured concentrations over periods of minutes to hours will reduce the noise spikes that are apparent in the concentration trends and should allow reliable time-weighted-average measurements of benzene vapors in the sub-parts-per-million range. Although not attempted here, these straightforward improvements should give this instrument the capability to monitor benzene in air at concentration levels specified by North American and European regulatory agencies such as NIOSH and OSHA.

By enabling real-time measurement of various molecular kinetics phenomena, this TDLAS instrument also offers useful features as a scientific tool. For example, future work can include evaluation of various sorbent materials for trapping ability and desorption efficiency. Future work can also include investigation of different catalytic surfaces designed to decompose benzene from waste streams. An interesting result from this work was that there was no improvement in the minimum detection limit of benzene when measurements were performed near the absorption

band peak in the 1953-cm⁻¹ spectral region (region B), as compared to when they were performed on the shoulder of this absorption band in the 1943-cm⁻¹ spectral region (region A). This can be explained by the fact that isolated rovibrational lines are not being measured. Instead, the measured absorption features, as shown in Figures 3 and 4, are combinations of very closely spaced rovibrational lines, and the spectral regions between the measured peaks contain weaker rovibrational absorption lines. The laser is thus measuring only small absorption variations on top of a larger unresolvable broad band absorption. Gas cooling methods, such as jet expansion, can greatly reduce the number of rovibrational lines, and this can theoretically allow significant improvements in detection sensitivities, since the signals for the remaining rovibrational absorption lines will be relatively much stronger. Implementing jet expansion techniques in a multipass White or Herriott cell would be difficult due to the large volume of optically sampled gas. However, it is possible to implement jet expansion gas cooling in smaller-volume gas cells designed for cavity ring down laser absorption spectroscopy, as recently demonstrated by Biennier et al.¹⁹ This combination of gas sampling and measuring techniques can help to expand greatly the capabilities of mid-infrared tunable laser absorption spectroscopy by enabling sensitive detection of large molecules that have spectrally dense rovibrational structure.

Results presented here also show that detection sensitivities can be improved by employing analyte trapping and desorption techniques. This is the same method employed by thermal-desorption GC/MS instruments to enhance detection sensitivities. In principle, minimum detection limits can be exceedingly small, in the parts-per-trillion range, if large amounts of air are passed through the activated carbon material and a rapid high temperature thermal desorption step is performed following analyte collection. Of course, such a TDLAS detection scheme will not provide real-time air monitoring results, but it will provide very high sensitivity with excellent analyte selectivity. The minimum amount of benzene that can be measured in the 107 m White cell is ~6 nmol, on the basis of the data in Table 2 and a 1 ppmv detection limit. Reducing this number to the picomolar range would allow this instrument to be used in some emerging gas analysis applications, such as exhaled biomarker measurement for early detection of diseases such as lung cancer.²⁰

The initial results and procedures reported here are still far from optimized. Better understanding of analyte trapping and the thermal desorption is needed, and further experiments can help achieve this. Data from the thermal desorption measurements summarized in Figure 7 and Table 2, for example, show that the gas cell pressure decreased as desorption temperature was increased, opposite of what is expected when more outgassing will occur at higher temperatures. This can be explained by the possibility of vapor leakage past a rubber septum in the thermal desorption cell during the desorption step. Pressure was allowed to build up in the desorption cell and surrounding fittings, since the valve to the gas cell was closed during this step. Higher desorption temperatures could cause more leakage due to higher pressures and more thermal expansion of the fittings. The smaller

than expected quantity of benzene for the 275 °C data point in the Figure 7 inset is consistent with this explanation. To prevent this, future thermal desorption measurements should involve rapid heating of the sorbent material while the valve to the gas cell is open.

Other significant issues also need to be understood better, such as the large difference between the amount of absorbed benzene and the amount released at high desorption temperatures. For example, it is known that 22.5 μmol of benzene was absorbed by the activated carbon, but a high desorption temperature of 275 °C released only 1.5 μmol into the gas cell. This low (6.7%) desorption efficiency may be explained by system leaks, benzene decomposition during the high-temperature thermal desorption step, physisorption on the glass wall and mirrors of the White cell, or analyte trapping at fittings and valves, etc. Improvement of this desorption (or extraction) efficiency number will help make a thermal desorption TDLAS instrument faster and more sensitive. Future research should thus focus on investigating sorbent materials that are optimized for specific analytes. Such work would be similar to the recent analysis of low-temperature glassy carbon-coated macrofibers, which showed an improvement in extraction efficiencies for various aromatic hydrocarbons when compared to commercial poly(dimethylsiloxane)/divinylbenzene (PDMS/DVB).²¹

Despite possible sources of measurement inaccuracy, the data points shown in Figure 10 are sufficiently linear to extract an activation energy for benzene desorption from carbon. The fact that the activated carbon was completely saturated with benzene before each desorption run likely contributed to the good results. The energy obtained, 19.0 kJ/mol, is believed to be the first reported experimental value for this phenomenon. This number compares very well with the activation energy of 17.6 kJ/mol reported for toluene desorption from activated carbon.²² These values are both much lower than the 53.6 kJ/mol activation energy for phenol desorption from activated carbon,²³ which should be expected, since phenol will be more "sticky" with its polar hydroxyl group.

CONCLUSIONS

A laser absorption spectrometer designed and built for detection of benzene vapor in the 5.1-μm spectral range was used to perform real-time measurements of benzene in a variety of air samples with a minimum detection limit of 1 ppmv. This sensitivity is more than 10 times better than the best prior TDLAS measurement of benzene vapor. Results showed excellent selectivity, as confirmed by monitoring multiple absorption features that were uniquely associated with the rovibrational absorption pattern for vapor phase benzene. Improvements in benzene sensitivity should be possible by employing jet expansion gas cooling to enhance rovibrational absorption lines or by employing analyte trapping and thermal desorption techniques. The autonomous operational capabilities of this software-controlled TDLAS instrument system can allow the system to operate for weeks at a time as an environmental pollution monitor without a human operator. In addition, the real-time, selective, and sensitive capabilities of this

(19) Biennier, L.; Salama, F.; Allamandola, L. J.; Scherer, J. J. *J. Chem. Phys.* **2003**, *118*, 7863.

(20) Phillips, M.; Gleeson, K.; Michael, J.; Hughes, B.; Greenberg, J.; Cataneo, R. N.; Baker, L.; McVay, W. P. *Lancet* **1999**, *353*, 1930–1933.

(21) Giardina, M.; Olesik, S. V. *Anal. Chem.* **2003**, *75*, 1604.

(22) Torrents, A.; Damera, R.; Hao, O. J. *J. Hazard. Mater.* **1997**, *54*, 141–153.

(23) Krebs, C.; Smith, M. *Chem. Eng. Sci.* **1985**, *40*, 1041–1050.

benzene sensor make it a useful tool for laboratory investigation of various kinetic phenomena.

ACKNOWLEDGMENT

This work was funded in part by USAF SBIR Grant no. 34601-01-0243. Technical guidance provided by Dr. Freddie Hall of the Environmental Management Directorate, Pollution Prevention

Division, at Tinker Air Force Base Air Logistics Center is gratefully acknowledged.

Received for review May 21, 2003. Accepted November 4, 2003.

AC0345392